Bioconjugate Chemistry

Article

pubs.acs.org/bc

Radiosynthesis and Preclinical Evaluation of 3′-Aza-2′-[^{18}F]fluorofolic Acid: A Novel PET Radiotracer for Folate Receptor Targeting

Thomas Betzel,[†] Cristina Müller,[‡] Viola Groehn,[§] Adrienne Müller,[†] Josefine Reber,[‡] Cindy R. Fischer,[†] Stefanie D. Krämer,[†] Roger Schibli,[†,‡] and Simon M. Ametamey*[,†]

[†]Department of Chemistry and Applied Biosciences, Institute of Pharmaceutical Sciences, ETH Zurich, Zurich, Switzerland

[‡]Center for Radiopharmaceutical Sciences ETH-PSI-USZ, Paul Scherrer Institute, Villigen-PSI, Switzerland

[§]Merck & Cie, Schaffhausen, Switzerland

Supporting Information

ABSTRACT: The folate receptor (FR) has been identified as a valuable target for the imaging of cancer and activated macrophages, involved in inflammatory and autoimmune diseases via positron emission tomography (PET). Therefore, conjugates of folic acid have been synthesized by coupling of a radiolabeled prosthetic group to the glutamate part of folic acid (pendent approach). In this work, we present a novel class of folates, where the phenyl ring of folic acid was isosterically replaced by a pyridine moiety for direct labeling with [^{18}F]fluoride (integrated approach). 3′-Azafolic acid and its 2′-halogenated derivatives (2′-chloro and 2′-fluoro) were evaluated in vitro to determine their binding affinity. 3′-Aza-2′-[^{18}F]fluorofolic acid ([^{18}F]**6**) was obtained, starting from N^2-acetyl-3′-aza-2′-chlorofolic acid di-*tert*-butylester (**2**), in a maximum decay corrected radiochemical yield of about 9% in ≥98% radiochemical purity and high specific activities of 35−127 GBq/μmol. Binding affinity to the FR was high (IC_{50} = 0.8 ± 0.2 nM), and the radiotracer was stable in human plasma over 4 h at 37 °C. No degradation or defluorination was detected after incubation of the radiotracer for 1 h at 37 °C with human and murine liver microsomes and human S9-fraction. In vivo PET imaging and biodistribution studies with mice demonstrated a high and specific uptake in FR-positive KB tumor xenografts (12.59 ± 1.77% ID/g, 90 min p.i.). A high and specific accumulation of radioactivity was observed in the kidneys (57.33 ± 8.40% ID/g, 90 min p.i.) and salivary glands (14.09 ± 0.93% ID/g, 90 min p.i.), which are known to express the FR and nonspecific uptake found in the liver (10.31 ± 2.37% ID/g, 90 min p.i.). Preinjection of folic acid resulted in a >85% reduced uptake of [^{18}F]**6** in FR-positive tissues (xenografts, kidneys, and salivary glands). Furthermore, no radioactive metabolites were detected in the blood, urine, or tumor tissue, 30 min p.i. These characteristics indicate that this new ^{18}F-labeled 3′-azafolate is an appropriate tool for imaging FR-positive (malignant) tissue.

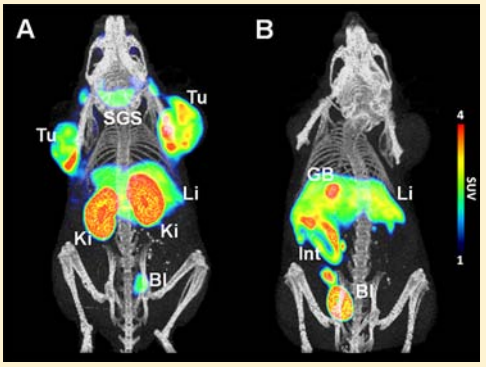

INTRODUCTION

The folate receptor (FR) is a 38−45 kDa membrane-associated glycoprotein, which binds folic acid with nanomolar affinity. The presence of the FR in healthy tissue is restricted to only a few organs and tissues such as the kidneys, lungs, salivary glands, placenta, and choroid plexus.[1] The FR-α isoform is overexpressed in specific types of human cancer, such as ovarian, cervical, endometrial, lung, kidney, and breast cancer.[1,2] The FR-β isoform shows a selective expression on activated macrophages, which are involved in inflammation and autoimmune diseases.[3,4] This selective upregulation of the FR in contrast to healthy tissue makes it a valuable target for the imaging of cancer and sites of inflammation.[5]

With regard to oncology, nine common cancer types show frequent FR overexpression.[1] Therefore, folic acid-based chemotherapeutic agents,[6−8] FR-α-targeted antibodies,[9] and antifolate drugs[10] have been developed for selective targeting of FR-positive cancer. For the imaging of FR-positive tumors, a variety of radiometal-based conjugates of folic acid have been investigated.[11−13]

Concerning inflammatory autoimmune diseases, 1% of the adult population worldwide is affected by rheumatoid arthritis, which makes it the most common inflammatory disease worldwide.[14] In order to treat this disease, folate conjugates of anti-inflammatory chemotherapeutic agents[15] or FR-β-targeted antibodies[16] are currently under investigation.

Therefore, there is an explicit need for noninvasive imaging agents, which allow the identification of patients who could benefit from FR-targeted therapy. The only FR-based radiotracer currently used in the clinic is ^{99m}Tc-EC20 (Etarfolatide, Endocyte Inc.), which is suitable for single photon emission computed tomography (SPECT).[17] In order to visualize small metastases and sites of inflammation, an ^{18}F-labeled PET

Received: August 30, 2012
Revised: December 18, 2012
Published: December 30, 2012

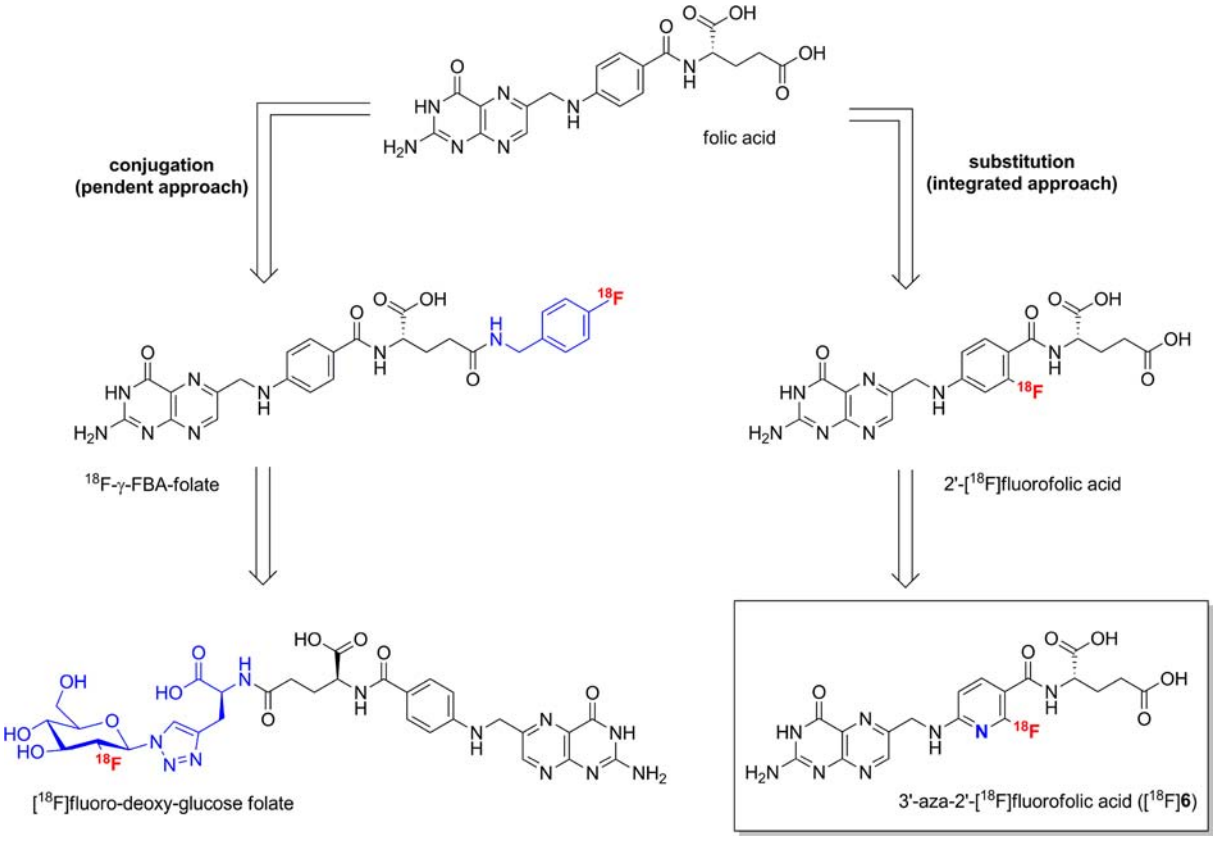

Figure 1. ^{18}F-Labeled folate radiotracers developed in our group following the pendent and integrated approach.

radiotracer could be more useful because it would benefit from improved imaging characteristics (resolution and sensitivity) due to the excellent positron decay characteristics of fluorine-18 ($E_{\beta^+,\max}$ = 0.6 MeV, $t_{1/2}$ = 109.8 min).

Our group developed the first ^{18}F-labeled folate radiotracer, ^{18}F-α,γ-4-fluorobenzylamine-folate (^{18}F-α,γ-FBA-folate), which was designed via conjugation with an ^{18}F-labeled prosthetic group (pendent approach).[18] FR-positive tumors were clearly visualized, but the uptake in nontargeted tissues was relatively high. As a further drawback, the prosthetic group was coupled nonselectively to both the α- and γ-carboxyl group of the glutamate moiety. To provide a single site-specific isomer, [^{18}F]fluoro-deoxy-glucose folate was synthesized by "clicking" 2-deoxy-2-[^{18}F]fluoroglucopyranosyl azide to a folate-γ-alkyne derivative.[19] This recently developed ^{18}F-folate radiotracer had a favorable radiochemical yield and showed excellent in vitro and in vivo characteristics. Other fluorine-18-based imaging probes have also been synthesized using the pendent approach, but a major drawback of all these ^{18}F-labeled folate conjugates is the complex and time-consuming multistep radiosynthesis, which renders translation to an automated synthesis system more cumbersome.[20,21]

A favorable alternative involving the direct attachment of the radionuclide to the folate backbone (integrated approach) was applied to the radiosynthesis of 2′-[^{18}F]fluorofolic acid.[22] The ^{18}F-label was introduced at the 2′-position of the phenyl ring by nucleophilic aromatic substitution of a nitro group. In vitro evaluation, small animal PET imaging, and biodistribution studies demonstrated favorable characteristics, but 2′-[^{18}F]-fluorofolic acid was obtained in a very low radiochemical yield of less than 4%, which is not optimal for clinical application. The structures of ^{18}F-labeled folate derivatives prepared by our group are shown in Figure 1.

To overcome the problems of multistep radiosyntheses and low radiochemical yields, we sought to replace the phenyl ring in folic acid with one less electron-rich pyridine ring. We reasoned that nucleophilic aromatic ^{18}F-fluorination at the 2′-position of the pyridine ring in 3′-azafolic acid would give a higher radiochemical yield without the need to introduce an activating group on the ring. Since it is known from the literature[23] that 2′- and 3′-azafolic acids have properties similar to those of native folic acid, we also hypothesized that using an azafolic acid backbone instead of folic acid would not affect FR-binding properties.

In this work, we present the synthesis of a new 3′-azafolate-based radiotracer, which still retains high affinity to the FR. We were able to produce 3′-aza-2′-[^{18}F]fluorofolic acid using an easy and reproducible two-step radiosynthesis with an increased radiochemical yield compared to 2′-[^{18}F]fluorofolic acid. Excellent in vitro and in vivo characteristics were obtained for this new folic acid derivative.

EXPERIMENTAL PROCEDURES

General. Reagents and solvents were purchased from Sigma-Aldrich Chemie GmbH, Acros Organics, and VWR International AG and used without further purification. For HPLC purification and analysis, a 50 mM sodium phosphate buffer at pH 7.4 was prepared (11.29 mmol/L $NaH_2PO_4 \cdot H_2O$ and 38.71 mmol/L $Na_2HPO_4 \cdot 2H_2O$).

Quality control of the radiolabeled compound was performed on an analytical Agilent 1100 series HPLC system, equipped with a 100 μL-loop and a GabiStar radiodetector (Raytest). An analytical HPLC column (Phenomenex, Luna PFP(2), C18, 5

dx.doi.org/10.1021/bc300483a | Bioconjugate Chem. 2013, 24, 205−214

Scheme 1. Syntheses of 3′-Azafolate Derivatives[a]

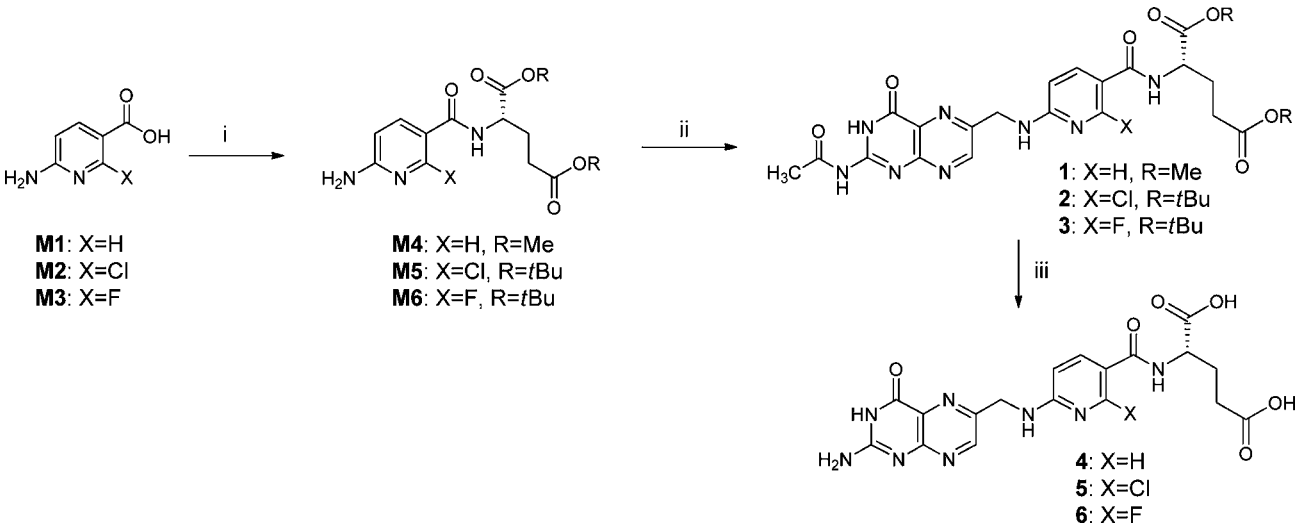

[a](i) (2*S*)-Glu(OR)OR·HCl with R = Me for compound **M4**, with R = *t*Bu for compounds **M5** and **M6**, HBTU, DMF, and Et_3N; (ii) N^2-acetyl-6-formylpterin, $NaBH(OAc)_3$, $Si(OEt)_4$ for **1** and **2**, molecular sieve 4A for **3**; (iii) 1 M NaOH for compound **4**, 1 M HCl for compounds **5** and **6**.

Scheme 2. Two-Step Radiosynthesis of 3′-Aza-2′-[^{18}F]fluorofolic Acid ([^{18}F]6)[a]

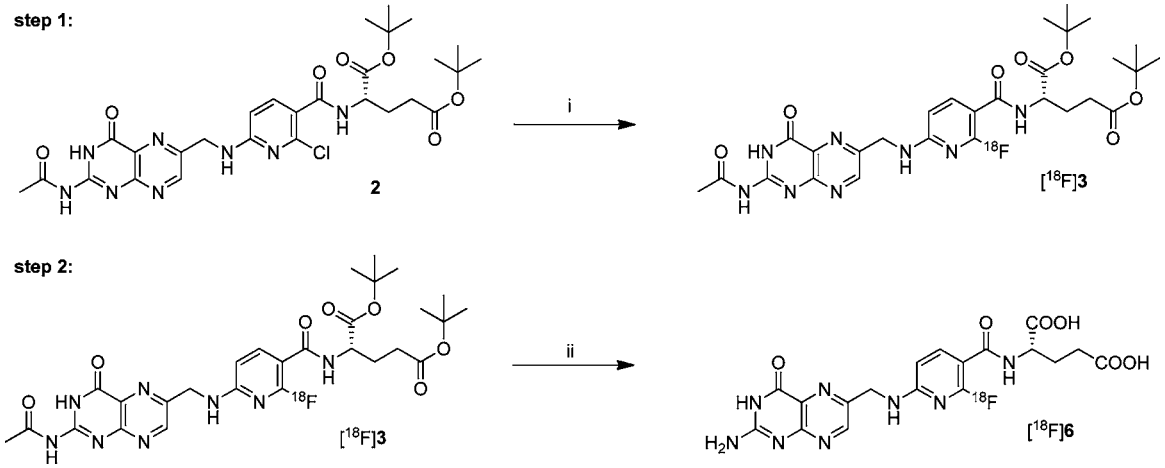

[a](i) [^{18}F]CsF-$K_{2.2.2}$, DMSO, 160 °C, 10 min; (ii) 4 M HCl, 60 °C, 10 min.

μm, 250 × 4.6 mm) was used at a flow rate of 1 mL/min with a gradient method, starting from 100% A to 30% B within 30 min (A = 50 mM sodium phosphate buffer; B = MeOH). UV absorption was recorded at 254 nm wavelength.

Specific activity was calculated based on the integrated UV peak by using a calibration curve, derived from different concentrations of the reference compound 3′-aza-2′-fluorofolic acid (**6**). Similarly, the amount of chlorinated compound **5** was determined by a standard curve, which was also obtained by the use of different concentrations.

Purification of the radiolabeled product was performed by using a semipreparative HPLC system, equipped with a Smartline Pump 1000, Smartline Manager 5000, Smartline UV detector 2500 (Knauer), 5 mL-loop, and a GabiStar radiodetector (Raytest). A semipreparative HPLC column (Phenomenex, Luna PFP(2), C18, 5 μm, 250 × 10 mm) was used at a flow rate of 4 mL/min with a gradient, starting from 100% A to 15% B within 10 min, followed by isocratic elution of the radioproduct from 10−25 min (t_R = 21 min) at 15% B (A = 0.1% EtOH in 50 mM sodium phosphate buffer; B = 40% EtOH in 50 mM sodium phosphate buffer). UV absorption was recorded at 254 nm wavelength.

Reaction control and analysis during stability studies were performed on an ultraperformance liquid chromatography system (UPLC, Waters), equipped with an Acquity UPLC column (Waters, BEH, C18, 1.7 μm, 2.1 × 50 mm) and a coincidence detector (Berthold, FlowStar LB513) at a flow rate of 0.6 mL/min with a gradient method, starting from 100% A to 60% B within 4.0 min (A = 50 mM sodium phosphate buffer; B = MeCN). [^{18}F]Fluoride incorporation yields were determined based on the radio-UPLC chromatograms.

Synthesis of 3′-Azafolate Derivatives. 3′-Azafolic acid (**4**), N^2-acetyl-3′-aza-2′-chlorofolic acid di-*tert*-butylester (**2**), which is the precursor for ^{18}F-labeling experiments, and the nonradioactive reference compounds, N^2-acetyl-3′-aza-2′-fluorofolic acid di-*tert*-butylester (**3**) and 3′-aza-2′-fluorofolic acid (**6**), as well as the deprotected precursor molecule, 3′-aza-2′-chlorofolic acid (**5**), were synthesized according to Scheme 1. Briefly, protected 3′-azafolic acid (**1**) was synthesized from commercially available 6-aminonicotinic acid (**M1**). Protected

dx.doi.org/10.1021/bc300483a | *Bioconjugate Chem.* 2013, 24, 205−214

3′-aza-2′-halofolic acid di-*tert*-butylesters (**2** and **3**) were obtained from 4-amino-2-halonicotinic acids (**M2**, **M3**). In the first step, the carboxylic acid group of the starting materials was activated with HBTU/triethylamine and coupled with the corresponding (2*S*)-glutamic acid diesters to give the *N*-(6-aminonicotinoyl)-(2*S*)-glutamates (**M4**, **M5**, and **M6**), which were used for reductive amination of N^2-acetyl-6-formylpterin. The amination reaction was achieved in acetic acid using a dehydrating agent and sodium triacetoxy borohydride as reducing agent. The N^2-acetyl-3′-azafolic acid dimethylester (**1**) and the N^2-acetyl-3′-aza-2′-halofolic acid di-*tert*-butylesters (**2** and **3**) were deprotected to give the corresponding 3′-azafolic acid derivatives (**4**, **5**, and **6**). Deprotection of compound **1** was achieved with 1 M NaOH at room temperature, whereas deprotection of compounds **2** and **3** was achieved by treatment with 1 M HCl at 60 °C.

Radiochemistry. Detailed information for [^{18}F]fluoride-cryptate preparation and radiosynthesis of the model compounds [^{18}F]**M6** and [^{18}F]**M7** are available in the Supporting Information. For the preparation of 3′-aza-2′-[^{18}F]fluorofolic acid ([^{18}F]**6**), the precursor N^2-acetyl-3′-aza-2′-chlorofolic acid di-*tert*-butylester (**2**) (2.50 mg, 3.96 μmol) was dissolved in anhydrous DMSO (300 μL) and added to the azeotropically dried [^{18}F]fluoride-cryptate complex (37−84 GBq) (Scheme 2). The solution was heated at 160 °C for 10 min and was allowed to cool down for 10 min. H_2O (5 mL) was added, and the solution was loaded on a Sep-Pak Plus tC18 cartridge (Waters, preconditioned with 5 mL of MeOH, followed by 10 mL of H_2O). Excess [^{18}F]fluoride was removed by rinsing the cartridge with H_2O (3 × 8 mL). The labeled intermediate, N^2-acetyl-3′-aza-2′-[^{18}F]fluorofolic acid di-*tert*-butylester ([^{18}F]**3**), was eluted with MeCN (2 mL) into another sealed Wheaton reactor (5 mL). MeCN was evaporated to near dryness under reduced pressure and a nitrogen stream at 90 °C. For deprotection, a 4 M HCl solution (1.25 mL) was added to the reaction vessel, and the solution was heated for 10 min at 60 °C to give [^{18}F]**6**. After cooling for 5 min, 5 M NaOH (1 mL) was added to neutralize the acidic solution, and thereafter, sodium phosphate buffer (2.5 mL) was added. The product was purified by semipreparative radio-HPLC. The product fraction was collected and passed through a sterile filter into a sterile and pyrogen-free vial. Chromatograms of the reaction mixture and HPLC analysis of the formulated radiotracer are available in the Supporting Information.

Cell Culture. KB cells (human cervical carcinoma cell line, HeLa subclone, ACC-136) were purchased from the German Collection of Microorganisms and Cell Cultures (DSMZ, Braunschweig, Germany). The cells were cultured as monolayers at 37 °C in a humidified atmosphere, containing 5% CO_2. Importantly, the cells were cultured in a folate-free cell culture medium, FFRPMI (modified RPMI, without folic acid, vitamin B_{12}, and phenol red: Cell Culture Technologies GmbH, Gravesano/Lugano, Switzerland). FFRPMI medium was supplemented with 10% heat-inactivated fetal calf serum (FCS, as the only source of folate), L-glutamine, and antibiotics (penicillin/streptomycin/fungizone). Routine culture treatment was performed twice a week after detachment with EDTA (2.5 mmol/L) in phosphate buffered saline (PBS).

In Vitro Binding Affinity Assays. ^{3}H-Folic acid (0.94 TBq/mmol) was purchased from Moravek Biochemicals Inc. Binding assays were performed with folic acid, 3′-azafolic acid (**4**), 3′-aza-2′-chlorofolic acid (**5**), and 3′-aza-2′-fluorofolic acid (**6**) on KB tumor cells. For the binding assay, a cell suspension in ice-cold FFRPMI medium (no additives, 7,000 cells in 240 μL per Eppendorf tube) was incubated in triplicate with ^{3}H-folic acid (0.82 nM) at increasing concentrations of the nonradioactive compound (5.0×10^{-12} to 5.0×10^{-7} M) at 4 °C for 30 min. Nonspecific binding was determined in the presence of excess folic acid (10^{-3} M). After incubation, Eppendorf tubes containing the cell suspensions were centrifuged at 1,000 rpm and 4 °C for 5 min, and the supernatant was removed. By addition of 1 M NaOH (500 μL), the cell pellets were lysed and transferred into scintillation tubes containing the scintillation cocktail (5 mL, Ultima Gold, Perkin-Elmer). Radioactivity was measured using a liquid scintillation analyzer (Tri-Carb 1900 TR, Packard), and the inhibitory concentration of 50% was determined by nonlinear regression analysis of displacement curves using GraphPad Prism (version 5.01) software.

Cell Uptake and Internalization. Cell uptake and internalization experiments were performed as previously described.[24] In brief, KB cells were seeded in 12-well plates to grow overnight (~700,000 cells in 2 mL of FFRPMI medium/well). The radiotracer, [^{18}F]**6** (200 kBq per well), was added to the cell monolayers. In some cases, cells were incubated with excess folic acid to block FRs on the surface of KB cells. After incubation at 37 °C for 1 or 2 h, cells were washed three times with PBS to determine total radiotracer uptake. In order to assess the fraction of radiotracer which was internalized, KB cells were additionally washed with a stripping buffer (aqueous solution of 0.1 M acetic acid and 0.15 M NaCl, pH 3) to release FR-bound radiotracer from the cell surface. Cell lysis was accomplished by the addition of 1 M NaOH (1 mL) to each well. The cell suspensions were transferred to 4 mL-tubes, and each sample was counted in a γ-counter. After homogenization by vortex, the concentration of proteins was determined for each sample by a Micro BCA Protein Assay kit in order to standardize the measured radioactivity to the average content of 0.3 mg of protein in a single well. The sum of FR-bound radiotracers and the internalized fractions were calculated as the percentage of total added radioactivity of the standard.

Determination of Distribution Coefficient. A saturated solution of phosphate buffer (1.74 g KH_2PO_4 and 9.60 g $Na_2HPO_4 \cdot 2H_2O$ in 1,000 mL of water, pH 7.4) in *n*-octanol and a saturated solution of *n*-octanol in phosphate buffer were prepared. [^{18}F]**6** (5 μL, 800 kBq) was added into an Eppendorf tube, containing buffer solution (500 μL) and *n*-octanol solution (500 μL). The Eppendorf tube was shaken for 15 min at room temperature, and the two phases were separated by centrifugation at 5,000 rpm for 3 min. An aliquot of each phase (150 μL) was transferred into an Eppendorf tube and counted in a γ-counter (Wizard, PerkinElmer). By calculating the logarithm of the ratio of the counts in the *n*-octanol and the phosphate buffer phase, the $\log D_{7.4}$ value was determined. Values represent the mean of 10 determinations from two independent experiments.

In Vitro Stability Studies. Detailed descriptions of the procedures on stability studies with human microsomes, murine microsomes, and glutathione/S9-fraction (glutathione-*S*-transferases) are available in the Supporting Information. For human plasma stability, the radiotracer [^{18}F]**6** was incubated for 4 h with human blood plasma at 37 °C. To test metabolism by hepatic microsomal enzymes, the radiotracer was incubated with human or murine microsomes for 1 h at 37 °C. In order to

assess the stability of [^{18}F]**6** toward degradation by glutathione, the radiotracer was incubated with glutathione and human liver S9-fraction for 1 h at 37 °C.

In Vivo Biodistribution Studies. All animal experiments were approved by the local veterinary department and complied with Swiss and local laws on animal protection.

Four to five week-old female, athymic nude mice (CD-1 Foxn-1/nu) were purchased from Charles River Laboratories (Sulzfeld, Germany). The animals were fed with a folate-deficient rodent diet (Harlan Laboratories) starting 5 days prior to tumor cell inoculation to reduce the serum concentration of folate to a level comparable to human serum levels.[25] Mice were inoculated with KB cells (5×10^6 cells) in PBS (100 μL) into the subcutis of each shoulder. Animal experiments were performed approximately 14 days after tumor cell inoculation. The animals were injected with [^{18}F]**6** (5 MBq in 100 μL of PBS) in the tail vein and sacrificed at variable time points (30, 60, and 90 min) postinjection (p.i.). For blocking studies, 10 min prior to radiotracer injection, a group of mice received excess folic acid in PBS (100 μg/100 μL) via intravenous tail vein injection. Mice were dissected, and selected organs and tissues were measured in a calibrated γ-counter (Wizard, PerkinElmer). The accumulated radioactivity was expressed as a percentage of the injected dose per gram of tissue (% ID/g), based on the effective injected total radioactivity.

In Vivo PET Imaging Studies. PET experiments were performed on an Explore VISTA PET/CT tomograph (GE Healthcare). Nude mice, bearing KB tumor xenografts on each shoulder were administered 10−18 MBq of [^{18}F]**6** formulations (100 μL per injection) via lateral tail vein injection (t = 0). To determine the specificity of the radiotracer, animals received excess folic acid in PBS (100 μg/100 μL) 10 min prior to the radiotracer injection in the tail vein. After injection of the radiotracer, mice were anesthetized by inhalation of isoflurane in an air/oxygen mixture approximately 5 min prior to PET data acquisition and scanned as described previously.[26] In dynamic PET mode, one animal was scanned from 0−90 min. For the second animal, data were acquired from 60−150 min p.i. Static PET scans were performed from 120−150 min p.i. as it was revealed to be the optimal time frame. After acquisition, PET data were reconstructed, and fused data sets of PET and CT were analyzed with PMOD software (version 3.3).

Metabolite Studies. For the determination of radiometabolites, [^{18}F]**6** (60−70 MBq) was intravenously injected into KB tumor bearing mice (n = 2). After 5 min, blood samples were taken from the opposite vein, and the animals were sacrificed 30 min after radiotracer injection. Blood, liver, tumor, and urine were collected. Blood samples were centrifuged at 5,000g for 5 min at 4 °C. The proteins of the plasma samples were precipitated by the addition of the same volume of ice-cold methanol followed by centrifugation. The supernatants of the plasma and the urine sample were diluted with phosphate buffer and analyzed by radio-UPLC. Liver and tumor tissue were homogenized in an equal volume of phosphate buffer using a PT 1200 C Polytron (Kinematica AG). After the addition of the same volume of ice-cold MeOH, the mixtures were centrifuged at 5,000g for 5 min and 4 °C. The supernatants were cleared from remaining proteins by the addition of ice-cold methanol, followed by centrifugation. The resulting supernatant fractions were diluted with phosphate buffer and analyzed by radio-UPLC.

RESULTS

Synthesis of 3′-Azafolate Derivatives. The synthesis of the precursor N^2-acetyl-3′-aza-2′-chlorofolic acid di-*tert*-butylester (**2**) was achieved in 2 steps in an overall yield of 38% starting from 2-chloro-6-aminonicotinic acid (**M2**). After cleavage of the protecting groups, 3′-aza-2′-chlorofolic acid (**5**) was isolated in 6% yield. The low yield for the deprotection step was due to repeated purification procedures, which were undertaken in order to obtain **5** in acceptable purity. N^2-Acetyl-3′-aza-2′-fluorofolic acid di-*tert*-butylester (**3**) was synthesized starting from 2-fluoro-6-aminonicotinic acid (**M3**) in an overall yield of 12%. Cleavage of the protecting groups afforded 3′-aza-2′-fluorofolic acid (**6**) in 56% yield. The three step synthesis of 3′-azafolic acid (**4**) starting from 6-amino-nicotinic acid (**M1**) was performed in an overall yield of 36% using dimethylester functionality for the protection of the glutamic acid moiety during the reductive amination reaction. A detailed description of the synthesis of all intermediates and final compounds including data for characterization will be published in a separate research article.

Radiosynthesis of 3′-Aza-2′-[^{18}F]fluorofolic Acid ([^{18}F]6). The radiosynthesis of [^{18}F]**6** was carried out in a two-step reaction. In a nucleophilic aromatic substitution, the chlorine-leaving group of compound **2** was replaced by [^{18}F]fluoride, followed by acidic removal of the protecting groups to give the final radiotracer [^{18}F]**6**. Up to 26% incorporation yield was accomplished for intermediate [^{18}F]**3** using DMSO as solvent at 160 °C for 10 min. The removal of the protecting groups under acidic conditions (4 M HCl, 60 °C) was complete within 10 min. However, an equal amount of a side product, [^{18}F]**M6**, was formed in the labeling step, which was also hydrolyzed ([^{18}F]**M7**). The side product was separated during semi-preparative radio-HPLC purification (t_R = 8 min). Also, the deprotected precursor molecule **5** (t_R = 19 min) was efficiently separated from the final product (t_R = 21 min). The radiotracer was obtained in an injectable physiological buffer solution in a decay-corrected overall yield of 3−9%. The total amount of radioactivity obtained for [^{18}F]**6** at the end of the synthesis (EOS) ranged from 0.93−2.87 GBq. Typically, 2 GBq of [^{18}F]**6** was obtained starting from 80 GBq [^{18}F]fluoride. Radiochemical purity was ≥98%, and the specific activity was 35−127 GBq/μmol after a total synthesis time of approximately 110 min. The chemical identity of [^{18}F]**6** was confirmed by HPLC by coelution with the nonradiolabeled reference compound **6**.

In Vitro Characterization. To investigate the potential influence of bioisosteric replacement of the phenyl ring of folic acid by a pyridine moiety, FR-binding affinity studies were performed with 3′-azafolic acid, using KB cells in a displacement experiment with ^{3}H-folic acid. We found that the affinity of 3′-azafolic acid was almost identical to that of folic acid (Table 1 and Figure 2 A). Also, FR-binding affinities of the 3′-aza-2′-halofolic acid reference compounds **5** and **6** were in the

Table 1. IC_{50} Values of Folic Acid, 3′-Azafolic Acid, 3′-Aza-2′-halofolic Acids, and 2′-Fluorofolic Acid

compd	IC_{50} (nM)
folic acid	1.1 ± 0.4
3′-azafolic acid (**4**)	1.3 ± 0.1
3′-aza-2′-chlorofolic acid (**5**)	0.8 ± 0.2
3′-aza-2′-fluorofolic acid (**6**)	1.4 ± 0.5
2′-fluorofolic acid[22]	0.9 ± 0.1

dx.doi.org/10.1021/bc300483a | *Bioconjugate Chem.* 2013, 24, 205−214

same range under the same experimental conditions (Table 1 and Figure 2 B).

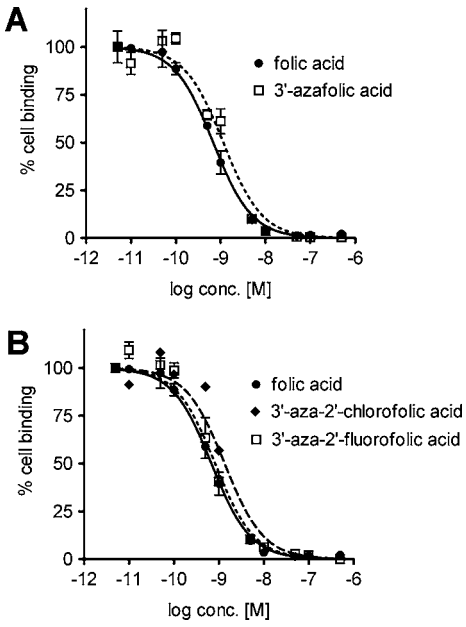

Figure 2. Graphs of displacement experiments for (A) folic acid and 3′-azafolic acid (**4**), and (B) folic acid, 3′-aza-2′-chlorofolic acid (**5**), and 3′-aza-2′-fluorofolic acid (**6**).

Cell Uptake and Internalization. The radiotracer [^{18}F]**6** was tested on KB tumor cells to determine FR-specific cell uptake and internalization. After 2 h of incubation at 37 °C, the uptake was about 78% (calculated per 0.3 mg of protein) of total added radioactivity, and the internalized fraction accounted for 19%. Co-incubation with excess folic acid resulted in an inhibition of radiotracer uptake to less than 1% (Figure 3).

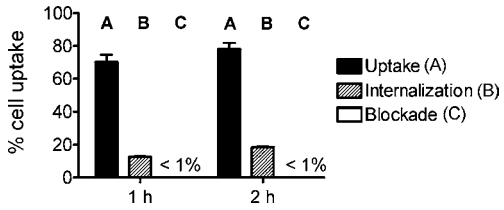

Figure 3. Uptake and internalization of [^{18}F]**6** and blockade studies with excess folic acid in FR-positive KB cells, incubated at 37 °C for 1 and 2 h.

Determination of Distribution Coefficient. The shake-flask method was applied to measure the distribution of [^{18}F]**6** in an octanol/water system under physiological pH conditions. The $\log D_{7.4}$ value was found to be −4.2 ± 0.1.

In Vitro Stability Studies. Incubation of [^{18}F]**6** with human blood plasma showed no degradation or defluorination of the radiotracer over a period of 4 h. The radiotracer was found to be completely stable when incubated with human and murine microsomes over 1 h. Also, incubation of the radiotracer with glutathione and human liver S9-fraction revealed no defluorination or radioactive degradation products of [^{18}F]**6** within 1 h (Figure 4).

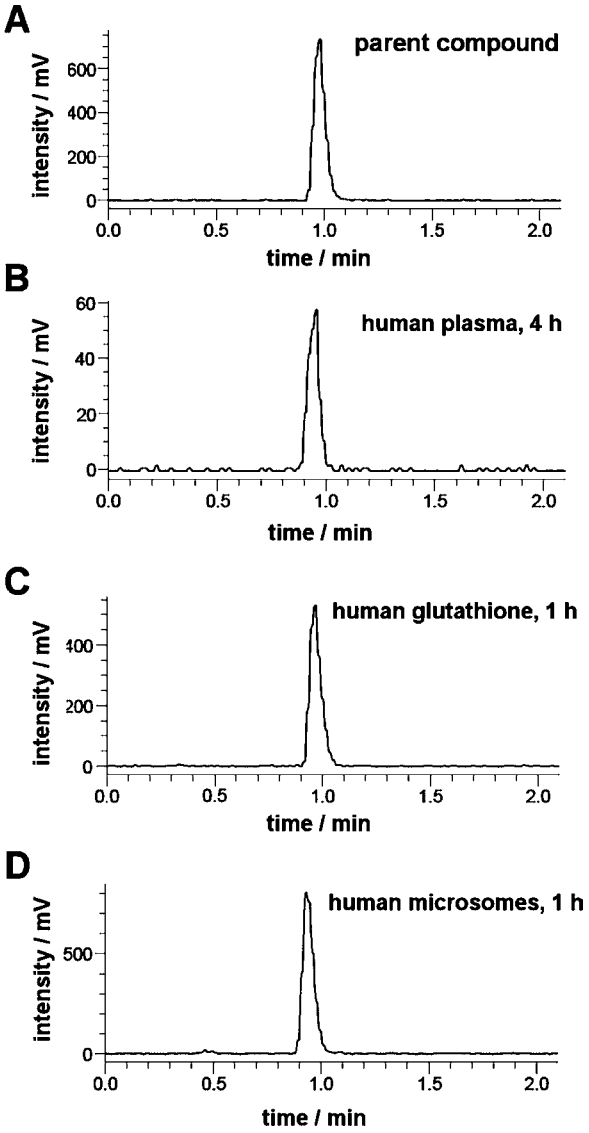

Figure 4. Radio-UPLC chromatograms of (A) parent compound ([^{18}F]**6**) and incubation of [^{18}F]**6** at 37 °C with (B) human blood plasma for 4 h, (C) human glutathione for 1 h, and (D) human microsomes for 1 h.

In Vivo Biodistribution Studies. The results of the biodistribution studies are listed in Table 2. Groups of mice (n = 4) were sacrificed at 30, 60, or 90 min p.i. The mice which received a preinjection of folic acid (n = 3) were sacrificed 60 min after [^{18}F]**6** injection. Radiotracer uptake in KB tumor xenografts showed an increase over time with a maximum uptake at 90 min p.i. (12.59 ± 1.77% ID/g). High uptake was also observed in the liver (10.3 ± 2.37% ID/g, 90 min p.i.) and in FR-positive tissues such as the salivary glands (14.09 ± 0.93% ID/g, 90 min p.i.) and the kidneys (57.33 ± 8.40% ID/g, 90 min p.i.). Already shortly after radiotracer injection, the amount of radioactivity in the blood was very low (1.15 ± 0.33% ID/g, 30 min p.i.) and decreased further over time (0.55 ± 0.06% ID/g, 90 min p.i.), indicating the fast clearance of [^{18}F]**6** from the blood pool. Only a negligible uptake of radioactivity was observed in the bones even at late time points (1.56 ± 0.32% ID/g, 90 min p.i.). The tumor-to-kidney ratios were low (~0.2) over the whole time of the investigation. Significantly reduced uptake (~85%) of the radiotracer in the

dx.doi.org/10.1021/bc300483a | *Bioconjugate Chem.* 2013, 24, 205−214

Table 2. Biodistribution Data of [^{18}F]6 in Nude Mice Bearing KB Tumor Xenografts

organ or tissue	30 min p.i. (n = 4)	60 min p.i. (n = 4)	90 min p.i. (n = 4)	60 min p.i. blockade[a] (n = 3)
		% ID/g in		
blood	1.15 ± 0.33	0.55 ± 0.07	0.55 ± 0.06	0.82 ± 0.30
heart	2.09 ± 0.21	1.89 ± 0.28	1.83 ± 0.10	0.39 ± 0.20
lungs	1.97 ± 0.31	1.52 ± 0.21	1.63 ± 0.27	0.72 ± 0.31
spleen	1.25 ± 0.23	1.85 ± 0.14	2.20 ± 0.16	0.37 ± 0.15
liver	13.72 ± 2.90	10.59 ± 0.89	10.31 ± 2.37	10.89 ± 3.39
gallbladder	8.10 ± 2.90	8.40 ± 1.79	9.26 ± 0.59	15.79 ± 9.28
kidneys	54.84 ± 6.10	53.60 ± 3.23	57.33 ± 8.40	5.89 ± 4.47
stomach	2.76 ± 0.45	2.83 ± 0.86	2.74 ± 0.04	0.61 ± 0.26
intestine	1.40 ± 0.14	1.90 ± 0.21	2.26 ± 0.40	1.93 ± 0.57
feces	1.23 ± 0.22	3.03 ± 1.98	1.77 ± 0.25	5.98 ± 1.08
salivary glands	9.00 ± 1.25	14.95 ± 6.09	14.09 ± 0.93	0.58 ± 0.21
bone	2.09 ± 0.32	1.57 ± 0.25	1.56 ± 0.32	0.57 ± 0.26
muscle	1.74 ± 0.38	1.24 ± 018	1.52 ± 0.38	0.33 ± 0.12
tumor	11.70 ± 0.87	11.86 ± 1.73	12.59 ± 1.77	1.74 ± 0.35
		Ratios		
tumor/liver	0.89 ± 0.24	1.13 ± 0.18	1.25 ± 0.35	0.16 ± 0.01
tumor/kidneys	0.22 ± 0.03	0.22 ± 0.02	0.21 ± 0.04	0.39 ± 0.21
tumor/blood	11.08 ± 4.11	21.58 ± 2.33	23.78 ± 4.09	2.19 ± 0.30

[a]Each animal received 100 μg of folic acid intravenously 10 min before the radiotracer injection.

tumor tissue (1.74 ± 0.35% ID/g, 60 min p.i.) was observed in mice that received excess folic acid. The same findings were observed for the kidneys where the uptake was reduced from 53.60 ± 3.23% ID/g (60 min p.i.) to 5.89 ± 4.47% ID/g (60 min p.i.).

In Vivo PET Imaging Studies. On the basis of quantitative analysis, dynamic PET scans revealed that [^{18}F]**6** uptake in the tumor was highest between 120 and 150 min p.i. Therefore, whole body PET scans were performed at 120−150 min p.i. Visualization of tumor xenografts was excellent since accumulation of radioactivity in nontargeted regions was generally low. Only the liver showed a relatively high amount of nonspecifically accumulated radioactivity. In the kidneys and salivary glands, FR-specific accumulation of the radiotracer was detected. In the mouse that received excess folic acid, the uptake of the radiotracer in the tumors, kidneys, and salivary glands was blocked, while increased uptake of the radiotracer was found in the intestinal tract and the liver (Figure 5).

Metabolite Studies. Analysis of plasma samples (5 and 30 min p.i.) as well as samples of urine and tumor 30 min after [^{18}F]**6** injection revealed no detectable amounts of radiometabolites. In contrast, analysis of the liver sample showed signs of metabolism (Figure 6).

DISCUSSION

The main goal of this work was to design a folate-based PET tracer with a good pharmacokinetic profile for the specific imaging of FR-positive tumors. A fast and robust radiosynthesis had to be developed, where the radiotracer could be obtained in a high and reproducible radiochemical yield, which is essential for a later translation of the radiotracer for clinical use. To achieve a higher radiochemical yield, we envisioned using a halo-precursor based on the rationale that halogens can easily be substituted into the 2′-position of the pyridine ring. Because of easy chemical accessibility, a precursor with a chloro leaving group was chosen. In vitro binding assays of 3′-azafolic acid demonstrated that substitution of the folic acid's phenyl ring by a pyridine moiety has no negative influence on FR-binding affinity. Furthermore, introduction of a halogen atom in 2′-position of the heterocyclic ring is also well tolerated with regard to FR-binding properties.

The positive results encouraged the synthesis of the precursor N^2-acetyl-3′-aza-2′-chlorofolic acid di-*tert*-butylester (**2**). (*S*)-Di-*tert*-butyl 2-(6-amino-2-chloronicotinamido)-pentanedioate (**M5**) is a key intermediate for the preparation of precursor compound **2**. To validate the radiolabeling strategy, compound **M5** was used as a model compound and successfully labeled with [^{18}F]fluoride to give [^{18}F]**M6**, which was hydrolyzed to [^{18}F]**M7**. Under optimized conditions, the model compound (**M5**) was labeled in a maximum yield of 56%, and the hydrolysis step was quantitative, indicating that 2′-chloro-3′-azafolate derivatives could be used as precursors for ^{18}F-labeling experiments.

The radiosynthesis of [^{18}F]**6** was carried out in an efficient two-step synthesis following the integrated approach via direct ^{18}F-labeling of precursor **2** and the subsequent cleavage of the protecting groups. Removal of unreacted [^{18}F]fluoride and cesium salts was accomplished by fast and efficient solid phase extraction. Only one HPLC purification step was necessary to obtain the final radiotracer in the desired chemical purity. The final purification step was challenging as the separation of the chlorinated from the ^{18}F-labeled 3′-aza-derivative was difficult. This problem could be solved by reducing the amount of precursor and the use of a pentafluorophenyl HPLC column.[27] The radiochemical yield was not significantly affected when the precursor amount was reduced. The choice of phosphate buffer and ethanol as HPLC mobile phase makes it possible to formulate the radiotracer in an injectable physiological solution, avoiding the steps of trapping and elution of the radiotracer on an additional cartridge. Besides the target compound [^{18}F]**6**, an equal amount of a radioactive byproduct was also formed. This byproduct was identified as [^{18}F]**M7**, a fragment of [^{18}F]**6**, which was generated by cleavage of the C−N bond that links the pteridine part of the molecule with the pyridyl glutamate entity during the radiolabeling procedure. It is known that folic acid is sensitive against irradiation[28] and that it may undergo photodegradation yielding 4-aminobenzoyl-L-glutamic acid and 6-formyl pterin.[29,30] Thus, the most likely reason for the

dx.doi.org/10.1021/bc300483a | Bioconjugate Chem. 2013, 24, 205−214

Figure 5. Maximum intensity projection of PET/CT in vivo scans of 30 min duration (120−150 min p.i.) performed with KB tumor-bearing mice of [^{18}F]**6**. (A) The scan of a mouse which received only the radiotracer (13 MBq), and (B) the scan of a mouse which received folic acid (100 μg) prior to the radiotracer (18 MBq). Tu = tumor, Li = liver, Ki = kidney, Bl = bladder, SGS = salivary glands, GB = gallbladder, and Int = intestine.

formation of [^{18}F]**M7** may be the harsh reaction conditions employed during radiosynthesis. The presence of compound **M5** as a possible source of impurity, which could potentially lead to the formation of [^{18}F]**M7**, can be excluded.

[^{18}F]**6** was obtained within 110 min in a maximum decay-corrected radiochemical yield of 9% in ≥98% purity, providing up to 2.9 GBq formulated radiotracer from 83.6 GBq starting activity. This amount of radioactivity would be enough for at least two patient studies. Although the total synthesis time of [^{18}F]**6** is comparable to that of 2′-[^{18}F]fluorofolic acid, the main advantage of [^{18}F]**6** is the higher and reproducible radiochemical yield when compared to that of previously developed ^{18}F-based folate radiotracers. With regard to a later transfer of the radiotracer production to an automated synthesis module, this aspect is of critical importance. A summary of the radiochemical yield of ^{18}F-labeled folate radiotracers accomplished so far in our group is given in Table 3. Detailed information about the yield of [^{18}F]**6** is provided in the Supporting Information.

Table 3. Overview of RCYs of ^{18}F-Labeled PET Folate Tracers

radiotracer	RCY of first step	RCY of second step	range of RCY of radiotracer after HPLC purification (decay corrected)[a]	total synthesis time
^{18}F-α,γ-FBA-folate[18]	max. 13%[b]	max. 44%[d]	1−6%	240 min
[^{18}F]fluoro-deoxy-glucose folate[19]	max. 75%[b]	quant.[d]	5−25%	180 min
2′-[^{18}F] fluorofolic acid[19,22]	max. 8%[c]	max. 50%[e]	1−4%	110 min
3′-aza-2′-[^{18}F] fluorofolic acid	max. 26%[c]	quant.[e]	3−9%	110 min

[a]On the basis of starting [^{18}F]fluoride radioactivity. [b]Synthesis of the ^{18}F-labeled synthon. [c]^{18}F-incorporation. [d]Coupling. [e]Deprotection.

In vitro cell uptake studies verified that [^{18}F]**6** was bound and internalized specifically in KB tumor cells. Stability experiments of [^{18}F]**6** in human and murine liver microsomes and human S9-fraction in the presence of excess glutathione as well as in human plasma showed no radioactive degradation products or defluorination but only intact parent compound. These findings indicate the high stability of [^{18}F]**6** against

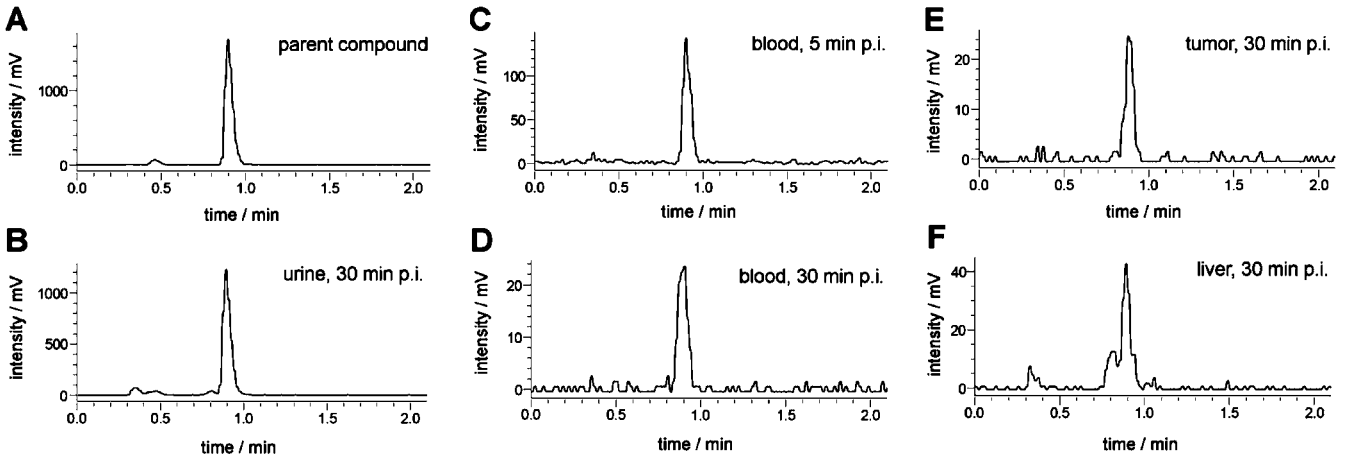

Figure 6. Radio-UPLC chromatograms of [^{18}F]**6** obtained from blood and different tissues after injection into a mouse. (A) Parent compound ([^{18}F]**6**), (B) urine 30 min p.i., (C) blood sample 5 min p.i., (D) blood sample 30 min p.i., (E) tumor 30 min p.i., and (F) liver 30 min p.i.

dx.doi.org/10.1021/bc300483a | *Bioconjugate Chem.* 2013, 24, 205−214

defluorination and toward hydrolases and oxidoreductases. Also, a further indication for high stability against defluorination is the negligible accumulation of radioactivity in the bones (1.56 ± 0.32% ID/g, 90 min p.i.), which was confirmed by in vivo biodistribution studies. The tumor uptake of [^{18}F]**6** (12.59 ± 1.77% ID/g, 90 min p.i.) is by far the highest when compared to that of other published ^{18}F-labeled folate derivatives: 6.56 ± 1.80% ID/g, 125 min p.i. for ^{18}F-α,γ-FBA-folate, 10.03 ± 1.12% ID/g, 60 min p.i. for [^{18}F]fluoro-deoxy-glucose folate, 9.37 ± 1.76% ID/g, 75 min p.i. for 2′-[^{18}F]fluorofolic acid, and 3.13 ± 0.83 ID/g, 45 min p.i for ^{18}F-click folate.[18−22,31] As expected, a high uptake of radioactivity was found in the kidneys as the FR is expressed in the proximal tubule cells. It serves as a physiologically important process to reabsorb folates from the primary urine and transport them back to the blood circulation by transcytosis.[32,33] Accumulation of radioactivity in the gallbladder and the feces in mice that received excess folic acid indicated a partial hepatobiliary excretion of the radiotracer. With regard to the tumor-to-background, tumor-to-liver, and tumor-to-kidney ratios, [^{18}F]**6** showed favorable characteristics that are comparable to those of our previously published ^{18}F-labeled derivatives.[19,22] Compared to [^{18}F]fluoro-deoxy-glucose folate and 2′-[^{18}F]fluorofolic acid, [^{18}F]**6** exhibited a reduced uptake in the abdominal region of mice. This represents a further advantage of the novel radiotracer [^{18}F]**6** as even small metastases or inflammatory sites could potentially be visualized in this region.

Metabolite studies of [^{18}F]**6** showed no radio-metabolites of the radiotracer in the urine, blood, and tumor 30 min after injection. Detectable amounts of radioactive metabolites were detected in liver tissue.

In summary, a radiotracer has been synthesized according to the integrated approach, which shows favorable in vitro and in vivo data comparable to those of [^{18}F]fluoro-deoxy-glucose folate but benefits from a fast and efficient radiosynthesis suitable for translation to a modular system for potential clinical application.

CONCLUSIONS

Our continuous efforts to develop folate-based PET radiotracers led to the radiosynthesis of 3′-aza-2′-[^{18}F]fluorofolic acid ([^{18}F]**6**), a novel radiotracer, which may serve as an appropriate diagnostic tool for imaging FR-positive diseased tissue. This radiotracer revealed favorable characteristics both in vitro and in vivo despite chemical modification of the folate backbone. Visualization of FR-positive tumors in mice was achieved with high image contrast and with only minor accumulation of radioactivity in nontargeted tissue. Compared to previously prepared ^{18}F-labeled folate-based radiotracers, the relative high yield as well as the fast and easy radiosynthesis of [^{18}F]**6** are major advantages. The translation of the radiosynthesis of [^{18}F]**6** to an automated synthesis module is currently in progress, and clinical studies are planned for the near future.

ASSOCIATED CONTENT

Supporting Information

High-resolution mass data, experimental details of radiolabeling, HPLC/UPLC analyses, and in vitro stability experiments. This material is available free of charge via the Internet at http://pubs.acs.org.

AUTHOR INFORMATION

Corresponding Author

*ETH Zurich, Wolfgang-Pauli-Str. 10, 8093 Zurich, Switzerland. Tel: +41 44 6337463. Fax: +41 44 6331367. E-mail: simon.ametamey@pharma.ethz.ch.

Notes

The authors declare no competing financial interest.

ACKNOWLEDGMENTS

We thank Nadja Romano, Claudia Keller, and Dominique Leutwiler for technical assistance. This work was financially supported by the Commission of Technology and Innovation, Switzerland (CTI 11667.1 PFLS-LS), in collaboration with Merck & Cie, Switzerland, and by the Swiss National Foundation (Ambizione Grant PZ00P3_121772).

REFERENCES

(1) Low, P. S., and Kularatne, S. A. (2009) Folate-targeted therapeutic and imaging agents for cancer. *Curr. Opin. Chem. Biol. 13*, 256−262.

(2) Parker, N., Turk, M. J., Westrick, E., Lewis, J. D., Low, P. S., and Leamon, C. P. (2005) Folate receptor expression in carcinomas and normal tissues determined by a quantitative radioligand binding assay. *Anal. Biochem. 338*, 284−293.

(3) Xia, W., Hilgenbrink, A. R., Matteson, E. L., Lockwood, M. B., Cheng, J.-X., and Low, P. S. (2009) A functional folate receptor is induced during macrophage activation and can be used to target drugs to activated macrophages. *Blood 113*, 438−446.

(4) Paulos, C. M., Turk, M. J., Breur, G. J., and Low, P. S. (2004) Folate receptor-mediated targeting of therapeutic and imaging agents to activated macrophages in rheumatoid arthritis. *Adv. Drug Delivery Rev. 56*, 1205−1217.

(5) Low, P. S., Henne, W. A., and Doorneweerd, D. D. (2007) Discovery and development of folic-acid-based receptor targeting for imaging and therapy of cancer and inflammatory diseases. *Acc. Chem. Res. 41*, 120−129.

(6) Li, J., Sausville, E. A., Klein, P. J., Morgenstern, D., Leamon, C. P., Messmann, R. A., and LoRusso, P. (2009) Clinical pharmacokinetics and exposure-toxicity relationship of a folate-vinca alkaloid conjugate EC145 in cancer patients. *J. Clin. Pharmacol. 49*, 1467−1476.

(7) Vlahov, I. R., and Leamon, C. P. (2012) Engineering folate-drug conjugates to target cancer: from chemistry to clinic. *Bioconjugate Chem. 23*, 1357−1369.

(8) Leamon, C. P., and Reddy, J. A. (2004) Folate-targeted chemotherapy. *Adv. Drug Delivery Rev. 56*, 1127−1141.

(9) Konner, J. A., Bell-McGuinn, K. M., Sabbatini, P., Hensley, M. L., Tew, W. P., Pandit-Taskar, N., Els, N. V., Phillips, M. D., Schweizer, C., Weil, S. C., Larson, S. M., and Old, L. J. (2010) Farletuzumab, a humanized monoclonal antibody against folate receptor α, in epithelial ovarian cancer: a phase I study. *Clin. Cancer Res. 16*, 5288−5295.

(10) Deng, Y., Wang, Y., Cherian, C., Hou, Z., Buck, S. A., Matherly, L. H., and Gangjee, A. (2008) Synthesis and discovery of high affinity folate receptor-specific glycinamide ribonucleotide formyltransferase inhibitors with antitumor activity. *J. Med. Chem. 51*, 5052−5063.

(11) Ke, C.-Y., Mathias, C. J., and Green, M. A. (2004) Folate-receptor-targeted radionuclide imaging agents. *Adv. Drug Delivery Rev. 56*, 1143−1160.

(12) Müller, C. (2012) Folate based radiopharmaceuticals for imaging and therapy of cancer and inflammation. *Curr. Pharm. Des. 18*, 1058−1083.

(13) Müller, C., and Schibli, R. (2011) Folic Acid conjugates for nuclear imaging of folate receptor-positive cancer. *J. Nucl. Med. 52*, 1−4.

(14) Stoll, J. G., and Yasothan, U. (2009) Rheumatoid arthritis market. *Nat. Rev. Drug Discovery 8*, 693−694.

(15) Lu, Y., Stinnette, T., Westrick, E., Klein, P., Gehrke, M., Cross, V., Vlahov, I., Low, P., and Leamon, C. (2011) Treatment of

experimental adjuvant arthritis with a novel folate receptor-targeted folic acid-aminopterin conjugate. *Arthritis Res. Ther. 13*, R56.
(16) Feng, Y., Shen, J., Streaker, E., Lockwood, M., Zhu, Z., Low, P., and Dimitrov, D. (2011) A folate receptor beta-specific human monoclonal antibody recognizes activated macrophage of rheumatoid patients and mediates antibody-dependent cell-mediated cytotoxicity. *Arthritis Res. Ther. 13*, R59.
(17) Fisher, R. E., Siegel, B. A., Edell, S. L., Oyesiku, N. M., Morgenstern, D. E., Messmann, R. A., and Amato, R. J. (2008) Exploratory study of ^{99m}Tc-EC20 imaging for identifying patients with folate receptor-positive solid tumors. *J. Nucl. Med. 49*, 899−906.
(18) Bettio, A., Honer, M., Müller, C., Brühlmeier, M., Müller, U., Schibli, R., Groehn, V., Schubiger, A. P., and Ametamey, S. M. (2006) Synthesis and preclinical evaluation of a folic acid derivative labeled with ^{18}F for PET imaging of folate receptor-positive tumors. *J. Nucl. Med. 47*, 1153−1160.
(19) Fischer, C. R., Müller, C., Reber, J., Müller, A., Krämer, S. D., Ametamey, S. M., and Schibli, R. (2012) [^{18}F]Fluoro-deoxy-glucose folate: a novel PET radiotracer with improved in vivo properties for folate receptor targeting. *Bioconjugate Chem. 23*, 805−813.
(20) Al Jammaz, I., Al-Otaibi, B., Amer, S., Al-Hokbany, N., and Okarvi, S. (2012) Novel synthesis and preclinical evaluation of folic acid derivatives labeled with ^{18}F-[FDG] for PET imaging of folate receptor-positive tumors. *Nucl. Med. Biol. 39*, 864−870.
(21) Al Jammaz, I., Al-Otaibi, B., Amer, S., and Okarvi, S. M. (2011) Rapid synthesis and in vitro and in vivo evaluation of folic acid derivatives labeled with fluorine-18 for PET imaging of folate receptor-positive tumors. *Nucl. Med. Biol. 38*, 1019−1028.
(22) Ross, T. L., Honer, M., Müller, C., Groehn, V., Schibli, R., and Ametamey, S. M. (2010) A new ^{18}F-labeled folic acid derivative with improved properties for the PET imaging of folate receptor-positive tumors. *J. Nucl. Med. 51*, 1756−1762.
(23) Roberts, E. C., and Shealy, Y. F. (1971) Folic acid analogs. Modifications in the benzene-ring region. 1. 2′- and 3′-Azafolic acids. *J. Med. Chem. 14*, 125−130.
(24) Müller, C., Mindt, T., de Jong, M., and Schibli, R. (2009) Evaluation of a novel radiofolate in tumour-bearing mice: promising prospects for folate-based radionuclide therapy. *Eur. J. Nucl. Med. Mol. Imaging 36*, 938−946.
(25) Mathias, C. J., Wang, S., Lee, R. J., Waters, D. J., Low, P. S., and Green, M. A. (1996) Tumor-selective radiopharmaceutical targeting via receptor-mediated endocytosis of gallium-67-deferoxamine-folate. *J. Nucl. Med. 37*, 1003−1008.
(26) Honer, M., Brühlmeier, M., Missimer, J., Schubiger, A. P., and Ametamey, S. M. (2004) Dynamic imaging of striatal D_2 receptors in mice using quad-HIDAC PET. *J. Nucl. Med. 45*, 464−470.
(27) Csató, E., Fülöp, N., and Szabó, G. (1990) Preparation of a pentafluorophenyl stationary phase for reversed-phase liquid chromatography. *J. Chromatogr. 511*, 79−88.
(28) Araujo, M. M., Marchioni, E., Bergaentzle, M., Zhao, M., Kuntz, F., Hahn, E., and Villavicencio, A. L. C. H. (2011) Irradiation stability of folic acid in powder and aqueous solution. *J. Agric. Food Chem. 59*, 1244−1248.
(29) Off, M. K., Steindal, A. E., Porojnicu, A. C., Juzeniene, A., Vorobey, A., Johnsson, A., and Moan, J. (2005) Ultraviolet photodegradation of folic acid. *J. Photochem. Photobiol., B 80*, 47−55.
(30) Vorobey, P., Steindal, A. E., Off, M. K., Vorobey, A., and Moan, J. (2006) Influence of human serum albumin on photodegradation of folic acid in solution. *Photochem. Photobiol. 82*, 817−822.
(31) Ross, T. L., Honer, M., Lam, P. Y. H., Mindt, T. L., Groehn, V., Schibli, R., Schubiger, P. A., and Ametamey, S. M. (2008) Fluorine-18 click radiosynthesis and preclinical evaluation of a new ^{18}F-labeled folic acid derivative. *Bioconjugate Chem. 19*, 2462−2470.
(32) Birn, H. (2006) The kidney in vitamin B12 and folate homeostasis: characterization of receptors for tubular uptake of vitamins and carrier proteins. *Am. J. Physiol. Renal. Physiol. 291*, F22−F36.
(33) Sandoval, R. M., Kennedy, M. D., Low, P. S., and Molitoris, B. A. (2004) Uptake and trafficking of fluorescent conjugates of folic acid in intact kidney determined using intravital two-photon microscopy. *Am. J. Physiol. Cell Physiol. 287*, C517−C526.